AD-A192 481 A CRITICAL REVIEW OF IR DROPS AND ELECTRODE POTENTIALS WITHIN PITS CREVIC..(U) PENNSYLVANIA STATE UNIV UNIVERSITY PARK DEPT OF MATERIALS SCI.. H W PICKERING

1/1

UNCLASSIFIED JAN 88 N00014-84-K-0201 F/G 7/4 NL

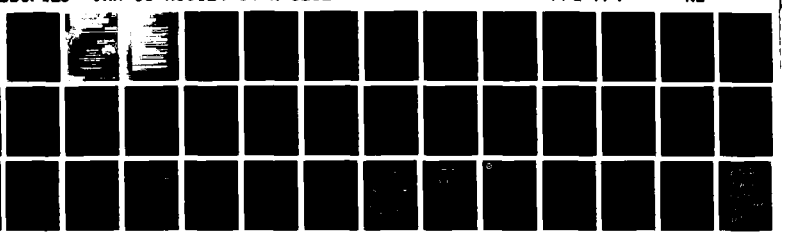

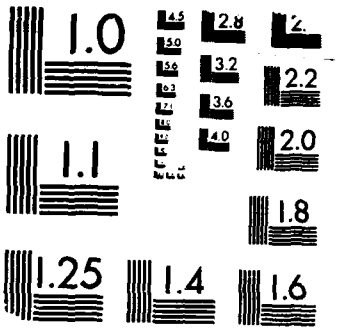


MICROCOPY RESOLUTION TEST CHART

AD-A1



88 2 17 008

[redacted]

SECURITY CLASSIFICATION OF THIS PAGE *(When Data Entered)*

| REPORT DOCUMENTATION PAGE | | READ INSTRUCTIONS BEFORE COMPLETING FORM |
|---|---|---|
| 1. REPORT NUMBER<br>Annual Technical Report | 2. GOVT ACCESSION NO. | 3. RECIPIENT'S CATALOG NUMBER |
| 4. TITLE *(and Subtitle)*<br>A Critical Review of IR Drops and Electrode Potentials within Pits, Crevices and Cracks | | 5. TYPE OF REPORT & PERIOD COVERED<br>Annual Technical Report |
| | | 6. PERFORMING ORG. REPORT NUMBER |
| 7. AUTHOR*(s)*<br>H. W. Pickering | | 8. CONTRACT OR GRANT NUMBER*(s)*<br>N00014-84-k-0201 |
| 9. PERFORMING ORGANIZATION NAME AND ADDRESS<br>Metallurgy Program, 209 Steidle Building<br>The Pennsylvania State University<br>University Park, PA 16802 | | 10. PROGRAM ELEMENT, PROJECT, TASK AREA & WORK UNIT NUMBERS |
| 11. CONTROLLING OFFICE NAME AND ADDRESS | | 12. REPORT DATE<br>January 1988 |
| | | 13. NUMBER OF PAGES |
| 14. MONITORING AGENCY NAME & ADDRESS*(if different from Controlling Office)* | | 15. SECURITY CLASS. *(of this report)* |
| | | 15a. DECLASSIFICATION/DOWNGRADING SCHEDULE |

16. DISTRIBUTION STATEMENT *(of this Report)*

17. DISTRIBUTION STATEMENT *(of the abstract entered in Block 20, if different from Report)*

18. SUPPLEMENTARY NOTES

19. KEY WORDS *(Continue on reverse side if necessary and identify by block number)*

20. ABSTRACT *(Continue on reverse side if necessary and identify by block number)*

The experimental data showing variations in electrode potential in actively growing pits, crevices and cracks are reviewed. Direct potential measurement, proton discharge within the local cell when thermodynamically unfavorable at the outer passive surface, faceting of the pit and crevice walls, and the presence of an active/passive boundary conclusively prove that pitting and crevicing of iron occurs when the electrode potential within the cell is below (less noble than) the Flade or passivation potential of the crevice

(over)

DD FORM 1 JAN 73 1473 EDITION OF 1 NOV 65 IS OBSOLETE
S/N 0102-014-6601

SECURITY CLASSIFICATION OF THIS PAGE *(When Data Entered)*

solution. Low pH and $Cl^-$ and other aggressive ions, are proposed to increase both the stability and rate of localized corrosion by increasing the size of the active loop and/or magnitude of the passive current of the cavity solution. The former decreases the magnitude of the required voltage drop (IR*) for the cavity electrode potential to be below the passivation potential and the latter increases the IR due to current flow out of the cavity, thereby providing for the necessary condition IR>IR* for localized corrosion. Ways in which passive film breakdown may occur, and pitting and crevicing commence, by this mechanism are identified.

Localized Corrosion Conference
Orlando, FL 1987

# A Critical Review of IR Drops and Electrode Potentials within Pits, Crevices and Cracks

H. W. Pickering

Department of Materials Science and Engineering
The Pennsylvania State University
University Park, PA 16802

ABSTRACT

The experimental data showing variations in electrode potential in actively growing pits, crevices and cracks are reviewed. Direct potential measurement, proton discharge within the local cell when thermodynamically unfavorable at the outer passive surface, faceting of the pit and crevice walls, and the presence of an active/passive boundary conclusively prove that pitting and crevicing of iron occurs when the electrode potential within the cell is below (less noble than) the Flade or passivation potential of the crevice solution. Low pH and $Cl^-$ and other aggressive ions, are proposed to increase both the stability and rate of localized corrosion by increasing the size of the active loop and/or magnitude of the passive current of the cavity solution. The former decreases the magnitude of the required voltage drop ($IR^*$) for the cavity electrode potential to be below the passivation potential and the latter increases the IR due to current flow out of the cavity, thereby providing for the necessary condition $IR>IR^*$ for localized corrosion. Ways in which passive film breakdown may occur, and pitting and crevicing commence, by this mechanism are identified.

## INTRODUCTION

Today's interest in potential variations within active local cells stems from the fact that potential as a parameter provides another approach to understanding the localized corrosion process. The well developed concepts of potential and current distribution coupled with the active/passive transition are the basis of the process. It is attractive for many reasons, not the least of which is its simple nature. It has the facility to explain the features of the simpler systems, i.e., those systems that do not have the requirement of acidification and/or aggressing ion buildup in the cavity solution, whereas when combined with these solution parameters it can explain the occurrence of localized corrosion in many, if not all, other systems.

An example is the crevicing of iron in buffered, slightly acidic solutions which are otherwise free of aggressive ions. In this case, it was found that the only necessary condition for localized corrosion of an otherwise anodically protected sample was that the electrode potential within the crevice was within the active loop region of the polarization curve of the crevice solution[1-3]. The composition of the crevice solution was essentially the same in pH as the bulk solution because of its buffering capacity and contained no $Cl^-$ or other aggressive ions since the bulk electrolyte contained none. Acidification and the addition of aggressive ions to these simpler systems further stabilizes and accelerates the crevicing process. The distribution of the potential and current in the cavity is determined in the same way it is on a finite planar electrode where ohmic drops and surface overpotentials are considered [4-6], and these concepts have been applied to localized corrosion and cathodic protection of crevices [7-9].

Another example is the pitting of iron in acid chloride solution [7], although pitting in this system has also been reported to occur in the absence of $Cl^-$ and other aggressive ions at elevated temperatures[10]. Here, too, a shift in electrode potential within the pit to a value in the Tafel or active region is known to be required[7].

The simplicity and attractiveness of the potential shift mechanism, which is not a new idea but is now strongly documented, comes from the fact that it is based on the active/passive transition. Thus, when the IR drop within the cavity is sufficient to place the cavity electrode potential below the passivation potential, $E_{pass}$, that part of the cavity will dissolve at a high rate while the rest of the surface is passive. This concept is illustrated in Figure 1. On the other hand, if $E_{pass}$ is far removed from the applied potential or, in the limit, no active region is apparent for the solution composition in the cavity as illustrated in Figure 2a, the condition IR>IR* is not met and modification of the solution composition, gas bubble accumulation on the surface or some other process is needed for localized corrosion to occur. Here, one couples the potential shift concept with a specific solution composition in the cavity (acidification and/or aggressive ion buildup) that decreases IR* (Figure 2b) or increases IR (by an increase in passive current), and/or with gas or solids on the surface that form microcrevices and, thereby, produce larger IR drops.[7,11] The consequence of decreasing IR* or of increasing IR is that the condition, IR>IR*, is met more easily and $i_{max}$ also may be larger, consistent with the known effects of acidification and/or aggressive ion buildup on increasing the rate of local cell processes, where IR* and $i_{max}$ are defined in Figure 1. The strong effects of $H^+$ and $Cl^-$ on the magnitudes of $E_{pass}$ and the passive current for corrosion resistant alloys are well documented in the corrosion literature. Some other results[12,13] are also consistent with this interplay of solution composition and the IR>IR* condition. For example, Stolica[12] observed sharp oscillations of the potential during early stages of pitting in galvanostatic experiments on Fe-Cr alloys in 1N $H_2SO_4$ containing small amounts of $Cl^-$, and increases in their frequency and magnitude with increase in the $Cl^-$ concentration. He and others[13] also considered that the pH effect was one of shifting $E_{pass}$.

If the premise that somewhere in the cavity the electrode potential is below its passivation or Flade potential during active crevicing or pitting is correct, which is

systematically documented below for iron and to some extent also for aluminum, stainless steel and titanium, the important question to ask is what are the conditions that place the cavity electrode potential below this transition ($E_{pass}$) potential. The answer to this question will be the focus of this paper, following a review of the experimental observations. The review will be restricted to the data and concepts relevant to a potential shift theory of localized corrosion and will not include the voluminous literature on the alternative and traditional acidification and aggressive-ion buildup mechanisms of localized corrosion that have received the preponderance of attention in the past, e.g., see the recent book by Sklarska-Smialowska.[14] It also will not include the roles of IR and hydrogen gas accumulation in cavities during cathodic polarization and cathodic protection of surfaces; although not comprehensive, reviews can be found elsewhere.[11,15,16]

## RESULTS

### Cavity Electrode Potential in the Tafel/Active Loop Region

The potential shift mechanism of stable localized corrosion is the outgrowth of two systematic studies of crevicing and pitting of iron[1-3,7] and a host of other related experimental and theoretical observations on different alloys.[11-13,17-24] This mechanism is also applicable to cracks according to several studies.[24-28] The recent study of Valdes[1-3] provided the important additional result that conclusively proved the occurrence of the potential shift mechanism when he showed that during active crevicing of iron (applied potential in the passive region) the crevice electrode potential was less positive than the Flade or passivation potential, $E_{pass}$, of the cavity solution. The active/passive interface could be clearly seen on the crevice wall of the iron sample and its position was followed and photographically recorded. This experimental observation is illustrated schematically for a crevice in Figure 1. Since a buffered solution free of aggressive ions was used in Valdes' work, it was, furthermore, concluded

that changes in composition were not necessary for stable crevicing to occur and that any that did occur were consequences rather than the cause of the local cell process, i.e., stability of a local cell is essentially just a matter of the cavity electrode potential having a value below the active/passive potential of the cavity solution whereas the outer surface is in the passive region. However, both acidification and aggressive ions have been found to increase stability and also the rates of crevicing[1-3,13] and pitting[7,10,12,14] of iron; this is in accord with a shift of $E_{pass}$ to more noble potentials, increases in $i_{max}$ of the active loop and increases in the passive current. Some of Valdes' experiments[1-3] also show that in a narrow, deep crevice gas bubble and/or solid-corrosion-product accumulation are not necessary for the condition IR>IR* to be met and for active crevicing to occur in the otherwise passivated sample.

Direct measurement of potential. Using fine Luggin capillary probes the local electrode potential in active pits and crevices can readily be measured. One such design that provides for precise movement of the probe in three directions within the cavity is shown in another paper of this proceedings[2] and is a modification of another design [7].

The measured difference between the inner and outer electrode potentials is typically $10^2$ to $10^3$ mV when the outer surface is anodically polarized into the passive region.[1-3,7,17-22,24-28] The condition $E<E_{pass}$ was found to hold in the cavity for different applied potentials to the sample, showing that the cavity electrode potential is largely independent of the outer surface potential, as found in several investigations of localized corrosion of iron[1-3,7], aluminum alloys,[24,25] steels,[26-28] and stainless steels[17,18]. And the cavity electrode potential decreases with distance into the cavity until the limiting potential, either a mixed potential or equilibrium potential of the metal dissolution reaction in the cavity which is a function of the composition of the cavity solution[11,23], is reached. This is best shown in the data of Valdes[1-3] for crevicing in iron, and the decrease was also seen in earlier data for pitting in iron[7].

Hence, the overpotential for metal dissolution decreases with increasing distance into the crevice and, hence so does the current below $E_{pass}$ as illustrated in Figure 1.

Conversely, for inactive local cells, the measured electrode potential within the cavity is close to the outer surface value[1-3,7]. Thus, activity of a local cell is found to be directly related to its electrode potential, as would be expected if the local potential mechanism is the correct explanation of localized corrosion: the local cell is active, i.e., growing by metal dissolution at high rates in the mA $cm^{-2}$ range when its electrode potential is less noble than the Flade or passivation potential of the cavity electrolyte, and inactive or passive with much lower dissolution rates in the $\mu A$ $cm^{-2}$ range when its electrode potential is near the outer surface potential in the passive region.

Other results of Valdes[1-3] consistent with these observations are as follows. For inactive crevices in iron, the crevice potential is in the passive region close to the value at the outer surface for both alkaline solutions free of chloride ions and for inhibited acid solutions. In addition, in the case of the alkaline solutions, when the solution in the cell is drained during the test and simultaneously filled with an acid solution, the potential in the crevice changes to the much more negative values of the Tafel region, and high rates of iron dissolution simultaneously commence in a region of the wall just below the active/passive interface. The electrode potential within the crevice and corresponding current response are shown in Figure 3. For the solutions used for obtaining the data in Figure 3, the change in potential of over one volt inside the crevice sometimes occurred in the short time of a few minutes after changing solutions. The experiment was conducted in the absence of accumulated gas or solid corrosion products in the crevice and in the absence of chloride ion in the test solution. The details of this and similar experiments involving inhibited solutions are presented elsewhere.[1-3] It was found that $IR^*$ is smaller for the acid (than alkaline) solution because of a more noble $E_{pass}$, allowing for the condition $IR>IR^*$ to be met. Similarly, in the case of the

inhibitor, IR* was found to be larger because of a less noble $E_{pass}$, in which case the condition IR>IR* was less readily met.

In these measurements the potential gradient in the cavity electrolyte was directly measured. As such, additional potential drops in corrosion product films, such as salt films, could even cause the total electrode potential difference to be larger than the measured values. In most of the measurements, however, film-potential drops must have been small or non-existent since the measured cavity electrode potentials were near the limiting electrode potential for the system.

Several other measurements of large potential differences between the inner cavity and other surfaces have been reported. Herbsleb and Engell[19], as early as 1961, reported that the inside of pits in iron anodically polarized in 0.5 M sulfuric acid - 0.3 mM sodium chloride has an electrode potential one volt negative of the outer passivated surface. France and Greene[17] and also Greene et al.,[18] measured potential drops in excess of one volt in crevices during anodic protection of stainless steel in 1 N sulfuric acid. Chen et al.[20] found a potential drop larger than one volt along a crevice in Ti-8Al-1Mo-1V in sulfuric acid solutions between one and ten normal and also in the presence of bromide and iodide ions. Davis[24] was one of the earliest who directly measured large potential drops in notches and cracks. He showed that the magnitude of the IR increased in an aluminum alloy exposed to a KCl aqueous solution of varying pH with increasing applied potential in both the anodic and cathodic directions. Others[25-28] have obtained similar results within cracks in steels and aluminum alloys, and have used these results as the basis of mechanisms of stress corrosion cracking and corrosion fatigue.

Hydrogen gas evolution from the cavity. The observation of hydrogen gas evolution from within active local cells when the hydrogen evolution reaction is thermodynamically impossible at the outer surface, is an independent proof of the existence of large potential differences between the inside and outside of actively growing

local cells. Careful experiments where there has been good control of the electrochemical conditions in order to insure that hydrogen evolution does not occur at the outer surface for the imposed conditions, have been carried out by Bargeron and Benson[22] who reported gas being evolved from pits in aluminum when the sample was anodically polarized at 1.02 V (SCE) in 1 M potassium chloride and identified it as hydrogen, by Pickering and coworkers[1-3,7], who observed a quasi stationary, continuous gas evolution from within pits and crevices in iron and stainless steel and identified it as hydrogen, and less conclusively (no control or measure of the external surface potential) by Forchhammer and Engell[21], who reported gas bubbles being evolved from pits in a stainless steel surface during elevated temperature exposure to neutral chloride solutions. In some of these experiments it was also clear that the hydrogen gas was coming from the electrolyte rather than from the metal itself.

Pickering and Frankenthal[7] observed in addition that the gas accumulated within the pit and that the accumulation led to the formation of large in-place hydrogen gas bubbles during pitting corrosion of iron and stainless steels. Based on this observation they proposed that accumulated gas in the cavity plays a major role in stabilizing pit and crevice growth by increasing IR and thereby facilitating the condition, IR>IR* and by developing the occulded cell condition. This observation provides one of the most credible explanations of how the electrode potential can vary by hundreds of mV over very short distances in the vicinity of the pit opening.

Faceting of local cell walls. In those cases where microscopic examination of the local cells were made, as in the early pitting experiments of Frankenthal and Pickering,[29] the walls of the pits at early stages were observed to be faceted. Valdes[1-3] also observed faceting and etching of crevice surfaces in iron whose outer surfaces were anodically polarized into the passive region. Faceting and etching are characteristics of dissolution in the Tafel region. Since the Tafel region does not usually extend to large overpotentials because of reaction product formation on the surface,

faceting is another evidence that the local electrode potential in actively growing cells is in the Tafel or active loop region of the polarization curve of the cavity electrolyte.

Crystallographic pits in a Ni surface that formed during anodic polarization at 0.76 V (SCE) have also been reported[30] and are evidence that the local electrode potential within the pits was in the Tafel region, i.e., much less noble than the applied 0.76 V (SCE). This explanation of the Ni result is the same as for the faceted structure in pits in iron. It is, however, contrary to the conclusions expressed by the authors of the Ni work.

**Rate of Localized Corrosion.**

A direct relation between the rate of metal dissolution and the electrode potential in the cavity is expected and is observed. An early documented evidence of this are the results of Pickering and Frankenthal.[7] They simultaneously measured the potential and current within pits in iron under conditions where the electrode potential in the pit was fluctuating with an amplitude of several hundred millivolts. Hence, the local electrode potential oscillated between active and less active or passive behavior. These potential spikes were matched exactly by spikes in the pitting current.

More recently, Valdes(1-3) has simultaneously measured the electrode potential in a crevice and the current flowing out of the crevice in iron exposed to solutions free of aggressive ions. The current was in the mA range when the electrode potential of the crevice was also in the Tafel/active loop region (pH 3 or 5 solutions), and was two or three orders of magnitude smaller when the local electrode potential in the crevice was near the outer surface potential in the passive region (pH 9 or 12 solutions). These results were obtained for iron samples anodically polarized at +600mV (SCE) and at other more positive potentials in the passive region.

When the above mentioned potential shift of over one volt from the passive to active range occurred in the crevice upon changing from a pH 9 or 12 to a pH 5 bulk solution (Figure 3a), a sharp increase of over two orders of magnitude in crevice current

occurred as shown in Figure 3b. Photographic recording of the crevice by the technique described elsewhere (1,2,31) showed that the crevice wall was completely passive for the duration of exposure to the alkaline solutions whereas within minutes after switching to the pH 5 solution, etching of the surface was visible below a distinguishing active/passive interface that developed part way into the crevice. After 24 minutes it was obvious that the highest rate of metal dissolution was occurring in a region just below the active/passive interface where the maximum current in the active loop occurs, as schematically illustrated in Figure 1. This rate can be even higher in the presence of an in-place gas bubble as is described in the next section. Valdes[1,3] also found that the rate of crevicing decreased with increasing applied potential in the range +600 to +900 mV (SCE).

**Gas Accumulation in the Cavity**

The potential profile in a crevice, in contrast to a pit, may not be significantly affected by the presence of an in-place gas bubble occupying the crevice cross section, according to recent results on iron by Valdes[1-3]. Typical profiles in the presence or absence of accumulated gas in the crevice used in his work are shown elsewhere in this proceedings.[2] The potential shift in the crevice was the same in the presence or absence of accumulated gas, and in the lower two-thirds of the crevice the electrode potential was within the Tafel/active loop region of the polarization curve of the crevice solution. This result indicates a lesser significance of accumulated gas in the case of crevicing of iron than for the case of pitting of iron where it was found that gas accumulation in the pit was necessary for pitting to occur.[7] The reason for this decreased importance is discussed below. On the other hand, accumulated gas may always accelerate the local cell process where the bubble contacts the metal surface, as reported in an earlier study[7] and now by Valdes[1-3]. For all other conditions the same, Valdes found that the crevicing current was over twice as high in the presence of gas accumulation.

In the absence of gas or solid-corrosion-product accumulation, the full cross section of the crevice is open to the bulk solution, and so it is straightforward to approximately calculate the IR drop due to current flow out of the crevice. The calculated values for the crevice dimensions and measured crevicing current agree well with the measured one volt IR drops. For the crevice opening used in the Valdes work (0.05 cm x 0.5 cm) and the measured current I, potential drop $\Delta E$ and depth L of the active/passive interface, typically 2 mA, 1V and 3mm, the conductivity of the crevice solution calculated using

$$k = IL/\Delta EA$$

is $2 \times 10^{-2}$ $ohm^{-1}$ $cm^{-1}$, indicating that $10^3$ mV IR drops can be readily supported by the existing conditions without invoking constrictions in the crevice.

One explanation for the higher crevicing current in Valdes' work when the crevice contained an in-place gas bubble is that the pH was lower in the crevicing solution in spite of its buffering capacity due to a more restricted mass transfer in and out of the crevice. This, in turn, would lead to a more pronounced active loop in the polarization curve of the crevice solution so that a higher metal dissolution rate would occur for any given $IR>IR^*$ value.

## DISCUSSION

There are two ways to explain the stability of localized corrosion processes, as shown in Figure 4. The traditional explanation proposes that the solution composition changes in the cavity rendering the passive film unstable. Once this condition is achieved, pitting or crevicing occurs since the cavity grows at a rate given by curve 1 while the outer surface corrodes at the passive rate for the electrode potential $E_s$ at the outer surface .

The second explanation or mechanism involves a shift of the electrode potential from $E_s$ at the outer surface to below the Flade or passivation potential, $E_{pass}$, within

the cavity where curve 2 represents the cavity solution and shows that it contains an active loop and passive region. In this explanation the electrode potential within the active pit or crevice is in the Tafel/active loop region of the polarization curve while the outer surface is at $E_s$. The rate of pit or crevice growth is given by currents in the active loop and will be higher at early times prior to the attainment of the lower stationary active loop values. In this case the solution composition again changes but in contrast to the first mechanism the change is largely, if not entirely, a consequence of both the different electrode potential in the cavity and the reaction products that form.

Hence, the experimental identification of acidification and/or chloride ion buildup in the cavity solution does not distinguish between these two basically different mechanisms. The parameter that can distinguish between them, however, is the electrode potential inside the cavity, in particular when coupled with information on the active/passive transition of the cavity electrolyte. Then, if IR>IR* so that $E < E_{pass}$, the second (local potential) mechanism is operative.

**Stability of the Local Cell Due to IR>IR***

Since the above described works[1-3,7] focused mainly on iron, the conclusions presented regarding the role of electrode potential on stability of the local cell can be applied to iron with some confidence. Certain of the observations have also been made for other metals, in particular the large measured and/or inferred (from the observation of $H_2$ gas) IR drops within pits, cracks and/or crevices of Al[22,24,25], Ti[20] and stainless steel[7,12,13,17,18] alloys. Stolica[12] and others also have found that certain pitting parameters, in particular the potential response, during galvanostatic experiments on Fe-Cr alloys have the same qualitative behavior as for iron.

There are, however, also many reports in the literature that do not directly test for potential changes within the cavity during localized corrosion, and interpretations of their data are done only on the basis of the changes in composition of the solution in the

cavity[14,32,33]. In some of these studies, various investigators have found that in systems of high $Cl^-$ ion concentration, the polarization curve of the bulk solution does not contain an active/passive transition, and on this basis they exclude the local potential concept in their explanations of the localized corrosion process. From potential theory, however, the local potential in the cavity is always less noble than the applied or outer surface potential for anodic polarization and/or open circuit corrosion conditions. These two potentials could be much different and it is important to know this difference, in order to quantitatively describe the kinetics of the local cell process in the presence (or absence) of an active/passive transition.

The minimum requirements for stable pitting or crevicing by the local potential mechanism are those needed to maintain the cavity electrode potential within the active loop of the polarization curve of the cavity electrolyte. Pickering and Frankenthal[7] proposed that the IR drop could be much larger than the calculated values that were based on an open or unconstricted cross section of the cavity and on the bulk solution resistivity. Their reasoning was based on the observation of gas bubble occupancy of the cross section of pits in iron and stainless steels, and on the potential probe measurements that showed that most of the potential change with increasing distance into the pits occurred in the vicinity of the accumulated gas.

In addition, Valdes[1-3] has found for relatively deep crevices that large, e.g., one volt, potential drops also regularly occur in the absence of gas accumulation. In this case, because of the relatively long solution path for current flow, the calculated IR drop of the unconstricted crevice using Eq. 1 is on the order of the measured values. Thus, a stable local cell can be maintained without the accumulation of gas because of the long current path which provides for $IR>IR^*$ within the crevice solution. In this case, as always, the composition of the cavity solution will change but this change can occur as a consequence of the potential difference and resulting local cell reactions. Although not

necessary for stability in such cases, these changes in solution composition will seemingly always significantly influence (increase) the rate of the local cell process.

It not for metal/solution systems such as Valdes' system which used an acidic buffered electrolyte free of aggressive ions, when are changes in solution composition necessary for stability? The answer to this question for the local potential mechanism seems logically to be when the IR>IR* condition is not otherwise met. In the pitting of iron at ambient temperatures when a particular electrode potential within the active loop is known to be required as mentioned above,[7-19] either or both acidification and aggressive ions are also required for growth and/or initiation in most situations. In the presence of a large buildup of $H^+$ ions in the cavity solution, its passivation potential is shifted to move noble values (IR* decreases) making the localized corrosion process more stable as the IR>IR* condition becomes easier to meet.

In Valdes' experiments[1-3], crevicing did not occur for the buffered pH 9 or 12 solutions, but did for the pH 3 and 5 solutions. It follows that if the buffer is removed from the pH9 and 12 solutions, active crevicing might be observed because the crevice solution undergoes acidification causing a shift of $E_{pass}$ in the noble direction and an increase in $i_{max}$ enabling E of the crevice to be below $E_{pass}$, ie.., a reduction in IR* and increase in IR making it easier for the IR>IR* condition to be met. Karlberg and Wranglen[13] have observed crevicing in ferritic stainless steels if the pH decreased and concluded it was for the same reason. In this situation both acidification and a more negative electrode potential in the crevice are necessary for stable crevicing.

Appreciable IR drops can be caused in different ways, as illustrated in Figure 5. The adjustable potential probe described elsewhere[1-3,7] works well for measuring IR drops in clear electrolyte, as well as in cases of gas accumulation and colloid formation, schemes 3 and 4 of Figure 5. It also can be effective when a perforated solid-corrosion product covers the cavity, but is largely ineffective for the measurement of IR drops within accumulated solid corrosion product because of the inability of the probe to

penetrate the solids. These latter two situations are shown in scheme 2 of Figure 5. For the same reason the probe is also ineffective for measuring IR in films adherent to the cavity surface as in scheme 1.

**In-Place Hydrogen Bubble Stability**

The finding that hydrogen gas accumulates and becomes a stable bubble within pits[7] was a really significant observation because it provided a plausible explanation of how the electrode potential within a small stably growing pit could be much less noble than that existing on the sample surface only a few μm away. As a corollary, by virtue of the microcrevice it forms with the sample surface, the attached gas bubble also can be the basis of an explanation for passive film breakdown and subsequent pit nucleation due to a lower electrode potential (below $E_{pass}$) in the microcrevice as discussed below. In-place gas bubbles have also been found to be instrumental for increasing the kinetics of the local cell process.[1-3,7] Thus, the in-place gas bubble is clearly more than a passing curiosity, and deserving of some discussion of its remarkable stability in spite of applied potentials that are hundreds of mV positive of that required to dissolve the bubble by hydrogen oxidation.

Its stability comes from the continuous generation of the gas in the deeper portions of the pit where the local electrode potential is more negative than the hydrogen equilibrium potential, as proposed before[7]. Thus, the reaction (in acid),

$$H^+ + e^- = 1/2\ H_2$$

occurs to the right in the deeper portions or the pit, whereas it occurs to the left in the outer portion of the pit where the electrode potential is strongly oxidizing to hydrogen gas. This situation is illustrated in Figure 6. At steady state both reactions occur at the same rate and the bubble size is fixed. Prior to steady state the bubble grows or wanes until the two rates are equal.

Another kind of bubble stability is its movement or lack thereof. Valdes[1-3] has observed that when the applied potential is switched from cathodic to anodic polarization,

an oscillary motion of the bubble decreases and the in-place lifetime of the bubble in the crevice actually increases. The explanation is not clear but a related observation was that the crevice solution became more viscous with time during anodic polarization. Greater viscosity is known to slow down transport processes of all types including motion of the bubble.

**Effect of the Crevice Width on IR/IR***

Because the IR product is affected by the cross sectional area of the crevice opening, its value will be a function of the width or narrowness of the opening. The relation for an approximate calculation is given in Eq. (1), which upon rewriting gives

$$IR = IL/kba$$

where a is the width or narrow dimension of the crevice and b is the length of the crevice. Thus, for all other quantities the same, an increase in the crevice gap, a, gives a reduced IR. From this consideration, one predicts that the active/passive interface should be deeper in the crevice and then disappear (i.e., the entire crevice wall passivates) as a increases.[11] This recently was experimentally found by Valdes[1], in agreement with the well known fact that crevicing only occurs for a below a certain value.

Actually, a detailed mathematical model has been completed some time ago which relates the IR drop to the a dimension of the crevice.[9] Although the model was developed for the specific process of hydrogen evolution on the crevice wall, the quantitative relation obtained between IR and a qualitatively applies to metal dissolution and other electrochemical reactions occurring on the crevice wall. Elsewhere in this Proceedings, Edwards[37] has reported the completion of such a model specifically for the crevicing process.

**Initiation Under the IR>IR* Condition**

There are two different situations to discuss in conjunction with the potential shift mechanism for the initiation of localized corrosion, and they provide different

complexities. The simpler, and one that could be referred to as a non-initiation event, involves surfaces that are free of a passive film at the moment of application of the potential $E_s$ in the passive region. Thus, on applying a potential in the passive region the current is initially high but immediately falls on the outer surface and also part way into the crevice as passivation occurs. Just below where IR=IR*, the current remains high and active crevicing is occurring (Figure 1). Valdes[1-3] has observed this initiation sequence for iron in experiments where either the sample was given a cathodic pretreatment and then the applied potential was switched to a value in the passive region or the sample was directly immersed with the applied potential in the passive region.

Another example for an initially film-free surface but where a constriction prevents passivation by enabling the IR>IR* condition to be met is when passivation occurs everywhere on a surface except where a gas bubble is attached to the surface. Presumably in this case the microcrevice that forms between the gas bubble and metal surface provides for the IR>IR* condition to be met, in which case pitting occurs where the bubble covers the metal. This has been observed by Valdes[1-3] for iron under the same conditions for which measurement of the potential in cavities routinely shows that the IR>IR* condition is the determining factor as to whether or not localized corrosion occurs.

The second more challenging situation involves breakdown of already passivated surfaces. Several possibilities exist here. One that has not been tested experimentally involves the attachment of a bubble on the surface followed by breakdown in the microcrevice region as above. In this case, the current flowing out of the microcrevice is only the passive current which, however, may increase with time due to gradual composition changes of the microcavity solution. Thus, the IR>IR* condition may be met so that thinning (dissolution) of the passive film occurs where the bubble covers the surface exposing the metal surface to the solution and permitting pitting to occur.

A similar situation may have been involved in the above described pH9 to pH5 solution-change experiment of Valdes[1-3]. When Valdes started with a pH9 or 12 solution causing the crevice wall to completely passivate and then switched to the pH5 solution, the crevice electrode potential changed, sometime rather quickly by hundreds of mV in the less noble direction, and the metal in this deeper one-half to three-quarters of the crevice was observed to dissolve indicating the passive film had dissolved. The metal dissolution rate in this portion of the crevice wall increased to values characteristic of active dissolution in a matter of minutes. In this case it was reasoned that the IR>IR* condition, although not met for the alkaline solutions, was more easily met for the acid solution because of its smaller IR* value ($E_{pass}$ shifts to more positive potentials as pH decreases) and larger IR values (the passive current is larger for the modified (thinner) passive layer of a pH5 solution) in which case $E<E_{pass}$ so that the passive layer in this deeper portion of the crevice dissolves followed by high rates of metal dissolution which stabilizes the IR>IR* condition to give active crevicing. The only difficulty with this reasoning is that the calculated IR drop, using Eq. 1, is too small using a typical passive current. It is, therefore, concluded that constrictions or some other process were operative in these experiments, such as an adherent gas bubble, in order to momentarily increase the magnitude of the voltage drops and meet the IR>IR* condition during the initiation process. Thus, a combination of film thinning permitting higher passive currents and bubble attachment were probably instrumental in the passive film breakdown and initiation of crevicing in this particular experiment.

Note that passive film breakdown in this case is the breakdown process associated with the normal sweep of the applied potential from the passive region into the active region, i.e., this breakdown process does not require special features usually invoked such as chloride adsorbtion or penetration of the film. Of course, a necessary pre-breakdown adsorption or absorption step may have been involved in this particular

experiment (although not $Cl^-$ ion since the solution contained none) in place of, or in addition to, a gas-bubble adsorbtion step as described next.

A third possibility which needs both theoretical and experimental analysis involves the interplay of the high field across the passive film with the absorbed species within the film, e.g., the reduction of $H_2O$ at the metal/passive film interface to form atomic hydrogen, hydrogen molecules or hydrogen bubbles at this interface. The physical presence of such reaction products in the layer as a result of this local "corrosion" process within the passive film, could affect the stability of the passive layer and lead to mechanical or chemical breakdown. If such a situation exists for proton discharge at the metal/film interface or elsewhere in the film because of the large voltage drop across the film which reduces or makes less noble the electrode potential at the metal/film interface, H and $H_2$ formation would likely occur at inhomogeneities in the metal/film interface including at second phase particles. Residual hydrogen in the metal (from the cathodic pretreatment or some other process) could also be involved in a similar way, in which case $H_2$ forms at the defects and mechanical degradation of the film occurs.

## CONCLUDING REMARKS

Experiments of the past fifteen years designed to evaluate the role of electrode potential in local cell processes have made a strong case for the pre-eminence of this parameter. A value of the electrode potential in the cavity that is less noble than the Flade or passivation potential, $E<E_{pass}$, appears to be essentially the sole factor determining the occurrence of localized corrosion of iron for some experimental conditions. As such, it is now concluded by some to be the basis generally of the localized corrosion process, be it pitting, crevicing or cracking. Thus, the local potential concept is based on a lower existing overpotential for metal dissolution in the cavity than exists on the external surface such that $IR>IR^*$ (Figure 1) placing the cavity surface in the Tafel or active region of the polarization curve of the cavity solution. Since the same

compositional changes occur in the cavity as with the traditional mechanisms, e.g., acidification and/or aggressive ion buildup (when aggressive ions are present), only measurement of the local cell potential can distinguish between potential shift mechanisms and other mechanisms. The presence of H+ and aggressive ions in the bulk solution increases both the likelihood that IR>IR* will be met and the rate of the crevicing process.

More systematic experiments are needed on the iron system to resolve remaining important questions, e.g., the relation between the pitting potential and the local cell potential, and unresolved details of the initiation process. Of course, the generality of the potential shift mechanism needs to be further investigated and unique aspects for each system resolved. In this regard there is now some experimental verification of the existence of significant potential variations within local cells in different technological alloy systems, not only in the case of the classical processes of pitting and crevicing but also for environmental cracking. In the areas of corrosion fatigue and to some extent stress corrosion cracking, recently developed models for steels and aluminum alloys include the potential variation as an important aspect of the mechanism.

ACKNOWLEDGMENT

Financial support by the Office of Naval Research under Contract No. N00014-84K-0201 is gratefully acknowledged.

## REFERENCES


1. A. Valdes, Ph.D. Thesis, The Pennsylvania State University, 1987.
2. A. Valdes and H. W. Pickering, "IR Drops and The Local Electrode Potential During Crevicing of Iron," this proceedings, page .
3. A. Valdes and H. W. Pickering, "El Potencial Local De Electrodo En Caridades, Fisuras Y. Grietas Y. Su Papel Como Cause Del Deterioro De Materials Estructurales," II Congress Iberoamericano De Corrosion Y-Proteccion, Maracaibo, Venezuela, NACE and the Latin American Association for Corrosion, 1986.
4. C. Wagner, J. Electrochem. Soc., Vol. 98, No. 3, p. 116, 1951.
5. J. Newman, J. Electrochem. Soc., Vol. 113, No. 5, p. 501, No. 12, p. 1235, 1966, ibid., Electroanal. Chem., Vol. 6, p. 187, 1973.
6. W. J. Albery and M. L. Hitchman, "Ring Disc Electrodes," Clarendon Press, Oxford, Chapter 4, 1971.
7. H. W. Pickering and R. P. Frankenthal, J. Electrochem. Soc., Vol. 119, No. 10, p. 1297, 1972: ibid., Localized Corrosion, R. W. Staehle, B. F. Brown, J. Kruger, A. Agrawal, Eds., National Association of Corrosion Engineers, Houston, Texas, p. 261, 1975.
8. J. Newman, Localized Corrosion, R. W. Staehle, B. F. Brown, J. Kruger, A. Agrawal, Eds., National Association of Corrosion Engineers, Houston, Texas, p. 45, 1975.
9. B. G. Ateya and H. W. Pickering, J. Electrochem. Soc., Vol. 122, No. 8, p.1018, 1975.
10. V. Mitgrovic-Scepanovic and R. J. Brigham, Corrosion Science, Vol. 27, No. 6, p. 545, 1987.
11. H. W. Pickering, Corrosion, Vol. 42, No. 3, p. 125, 1986.
12. N. Stolica, Corrosion Sci., Vol. 9, p. 205, 1969.
13. G. Karlberg and G. Wranglen, Corrosion Sci., Vol. 11, p. 499, 1971.

14. Z. Sklarska-Smialowska, Pitting Corrosion of Metals, National Association of Corrosion Engineers, Houston, 1986.

15. H. Pickering, "Role of Gas Bubbles and Cavity Dimensions on the E-pH-Ion Concentrations inside Cavities," in Equilibrium Diagrams Localized Corrosion, R. P. Frankenthal and J. Kruger, Eds., The Electrochemical Soc., Inc., Pennington, N.J., p. 535, 1984.

16. H. W. Pickering and A. Valdes, "A Review of the Effect of Gas Bubbles and Cavity Dimensions on the Local Electrode Potential Within Pits, Crevices and Cracks," in Embrittlement by the Localized Crack Environment, R. P. Gangloff, ed., Metallurgical Soc. of AIME, Warrendale, PA p. 33, 1984.

17. W. D. France and N. D. Greene, Corrosion, Vol. 24, No. 8, p. 247, 1968.

18. N. D. Greene, W. D. France, Jr., B. E. Wilde, Corrosion, Vol. 21, No. 9, p. 275, 1965.

19. G. Herbsleb and H. J. Engell, Z. Elektrochem., Vol. 65, NO. 10, p. 881, 1961.

20. C. M. Chen, F. H. Beck, M. G. Fontana, Corrosion, Vol. 27, No. 6, p. 234, 1971.

21. P. Forchhammer, H. J. Engell, Werkst, Korros., Vol. 20, No. 1, p. 1, 1969.

22. C. B. Bargeron and R. C. Bensen, J. Electrochem. Soc., Vol. 127, No. 11, p. 2528, 1980.

23. H. W. Pickering, H. H. Uhlig, Symp. Corrosion and Corrosion Protection, R. P. Frankenthal, F. Mansfeld, Eds., Electrochemical Society, Pennington, NJ, p. 85, 1981.

24. J. A. Davis, "Use of Microelectrodes for Study of Stress Corrosion of Aluminum Alloys," in Localized Corrosion, R. W. Staehle et al., eds., NACE, Houston, TX, p. 168, 1975.

25. R. A. H. Edwards, "Potential Drop and Concentration Changes in Stress Corrosion Cracks in 7075 Alloy in Halide Solutions," in Corrosion and Exploitation of the

Corrosion of Aluminum Alloys, Holroyd, Scamens and Fields, Eds., Alcon International, 1984.

26. A. Turnbull and M. K. Gardner, British Corrosion, J., Vol. 16, No. 3, p. 140, 1981.

27. R. A. H. Edwards and P. Schuitemaker, "Determination of Crack Tip pH and Electrode Potential during Corrosion Fatigue of Steels", in Corrosion Chemistry within Pits, Crevices and Cracks, A. Turnbull, Ed., Her Majesty's Stationery Office, London, p. 453, 1987.

28. K. Landles, J. Congleton, and R. N. Parkins, "Potential Measurements Along Actual and Simulated Cracks", in Corrosion Chemistry within Pits, Crevices and Cracks, A. Turnbull, Ed., Her Majesty's Stationery Office, London, p. 453, 1987.

29. R. P. Frankenthal and H. W. Pickering, J. Electrochem. Soc., Vol. 119, No. 10, p. 1304, 1972.

30. H. H. Strehblow and M. B. Ives, Corros. Sci., Vol. 16, No. 5, p. 317, 1976.

31. D. Harris and H. W. Pickering, "On Anodic Cracking During Cathodic Hydrogen Charging", in Effect of Hydrogen on the Behavior of Materials, A. W. Thompson, I. M. Bernstein and A. J. West, eds., Metallurgical Soc. of AIME, Warrendale, PA p. 229, 1976.

32. G. T Gaudet, W. R. Mo, T. A. Hatton, J. W. Tester, J. Tilly, H. S. Isaacs and R. C. Newman, American Chem. Engr. J., Vol. 32, No. 6, p. 949, 1986.

33. J. W. Tester and H. S. Isaacs, J. Electrochem. Soc., Vol. 122, No. 11, p. 1438, 1975.

34. A. Turnbull and J. G. N. Thomas, J. Electrochem. Soc., Vol. 129, No. 7, p. 1412, 1982.

35. N. J. H. Holroyd and M. R. Jarrett, "Solution Chemistry Within Pits, Cracks and Crevices in Aluminum Alloys," this proceedings, p .

36. R. A. Cottis, A. Alavi and E. T. Taai, "Chemical Conditions and Hydrogen Generation Within Crevices in Carbon-Manganese Steels", this proceedings, p. .

37. R. A. H. Edwards, "A Simple Mass Transport Analysis of Localized Corrosion," this proceedings, p. .

## FIGURE CAPTIONS

Figure 1. Schematic illustrating the relation between the local cell area in the crevice and the polarization curve of the crevice solution for a sample polarized to potential A in the passive region. The nonpassivated area deeper into the crevice (below $E_{lim}$) is at the mixed potential of the cavity solution.

Figure 2. Schematic illustrating a decrease in $IR^*$ due to development/enlargement of the active loop by a change in concentration of the cavity solution.

Figure 3. Potential and current transients inside a crevice in Fe before and after changing from the pH 9 to the pH 5 solution. Both solutions were buffered and free of aggressive ions, and the sample was anodically polarized in the passive region at 600 mV (SCE).

Figure 4. Schematic polarization curves of the cavity electrolyte for the traditional mechanism (curve 1) and the potential shift mechanism (curve 2).

Figure 5. Schematic illustrating the different forms of constriction affecting the IR drop in the cavity. The application of a potential measuring probe for these different situations is discussed in the text.

Figure 6. Schematic illustrating the relation between the polarization curves and the dynamic (chemical) stability of an inplace hydrogen gas bubble in the crevice. Increased solution viscosity also contributes to the (mechanical) stability.

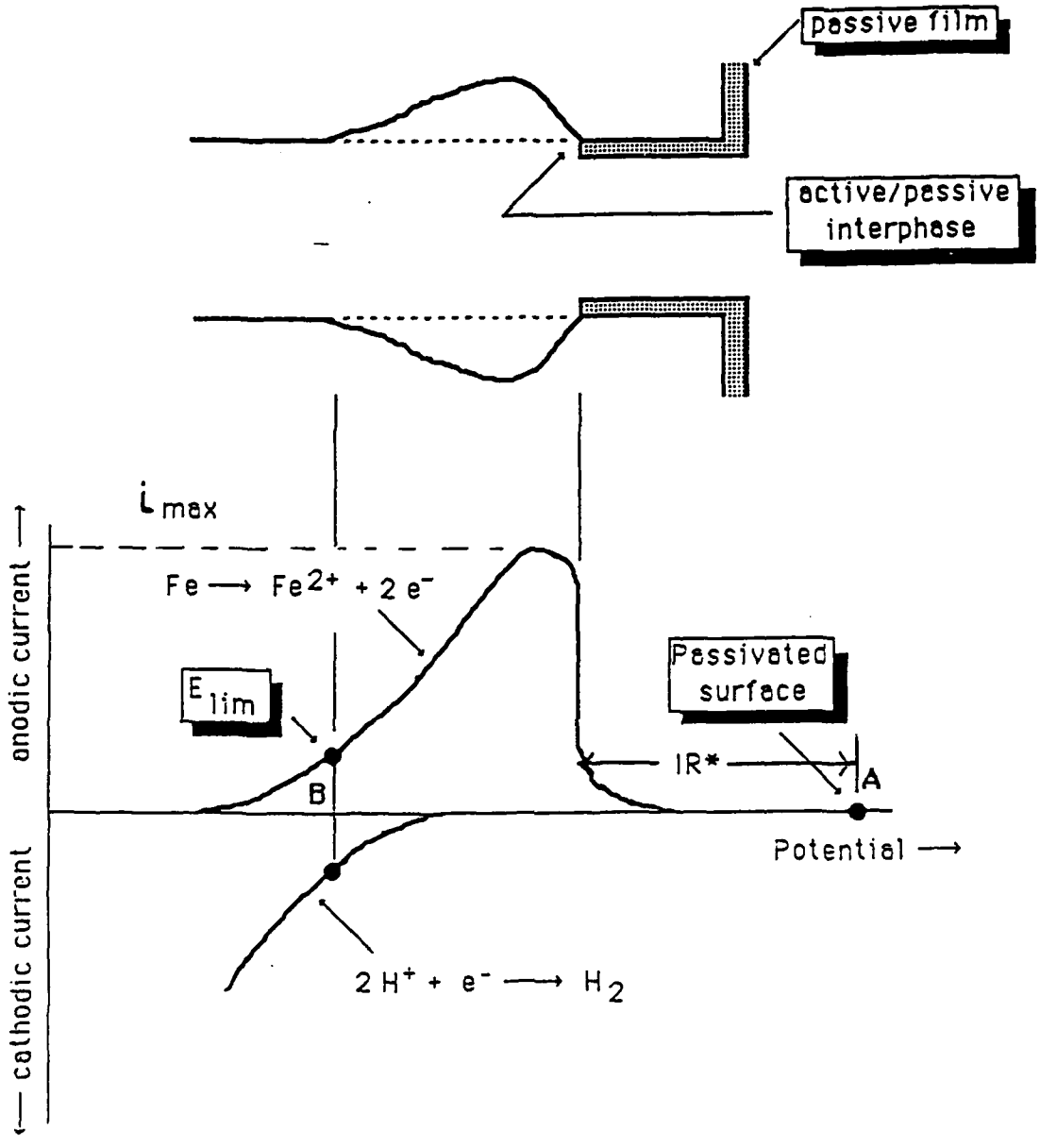


Figure 1. Schematic illustrating the relation between the local cell area in the crevice and the polarization curve of the crevice solution for a sample polarized to potential A in the passive region. The nonpassivated area deeper into the crevice (below $E_{lim}$) is at the mixed potential of the cavity solution.

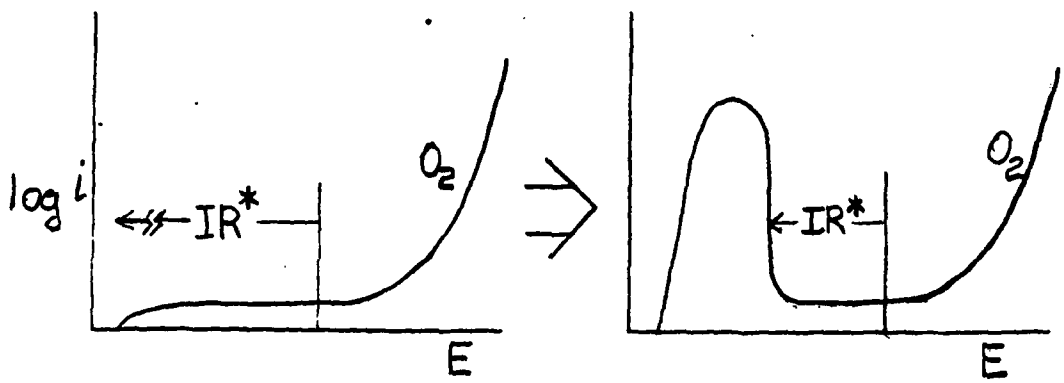


Figure 2. Schematic illustrating a decrease in IR* due to development/enlargement of the active loop by a change in concentration of the cavity solution.

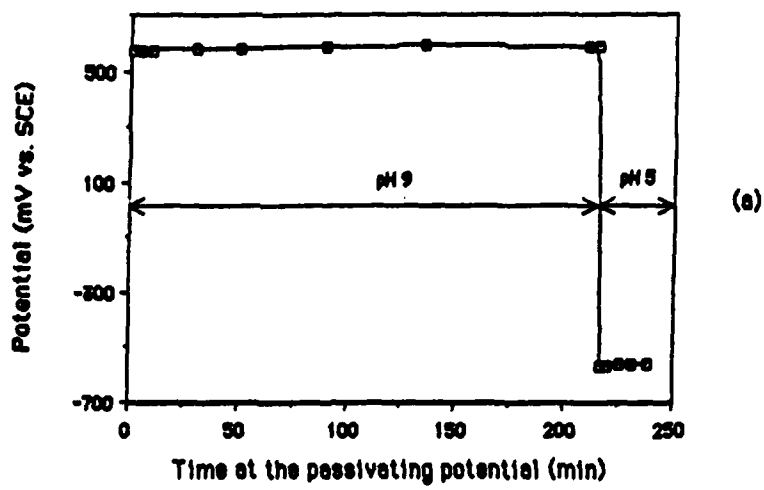


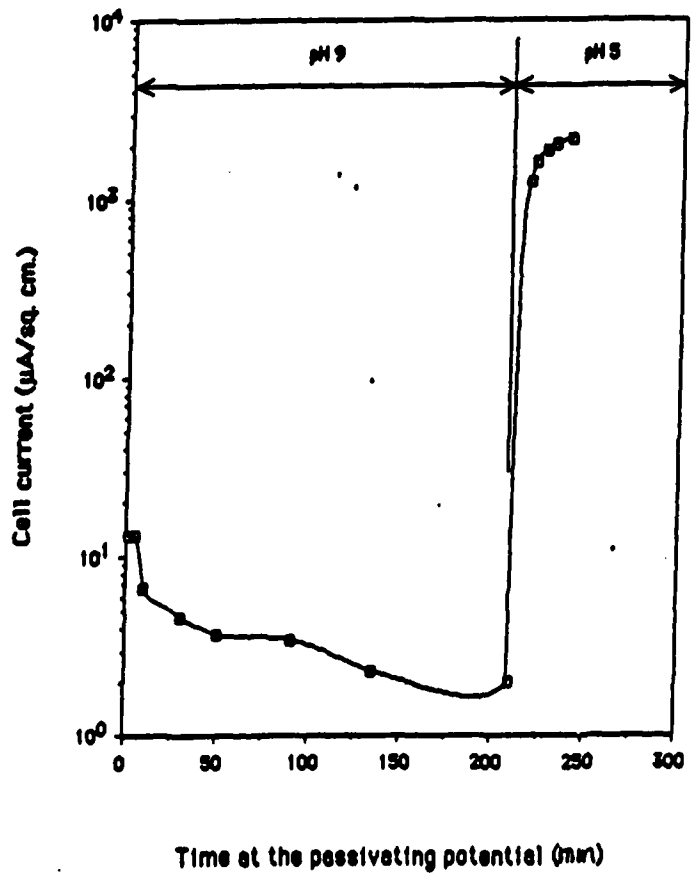


Figure 3. Potential and current transients inside a crevice in Fe before and after changing from the pH 9 to the pH 5 solution. Both solutions were buffered and free of aggressive ions, and the sample was anodically polarized in the passive region at 600 mV (SCE). After Valeo[1].

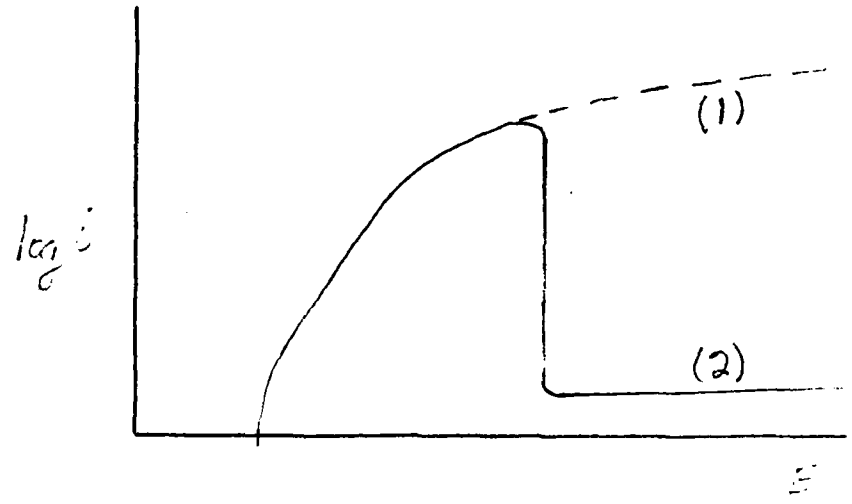


Figure 4. Schematic polarization curves of the cavity electrolyte for the traditional mechanism (curve 1) and the potential shift mechanism (curve 2).

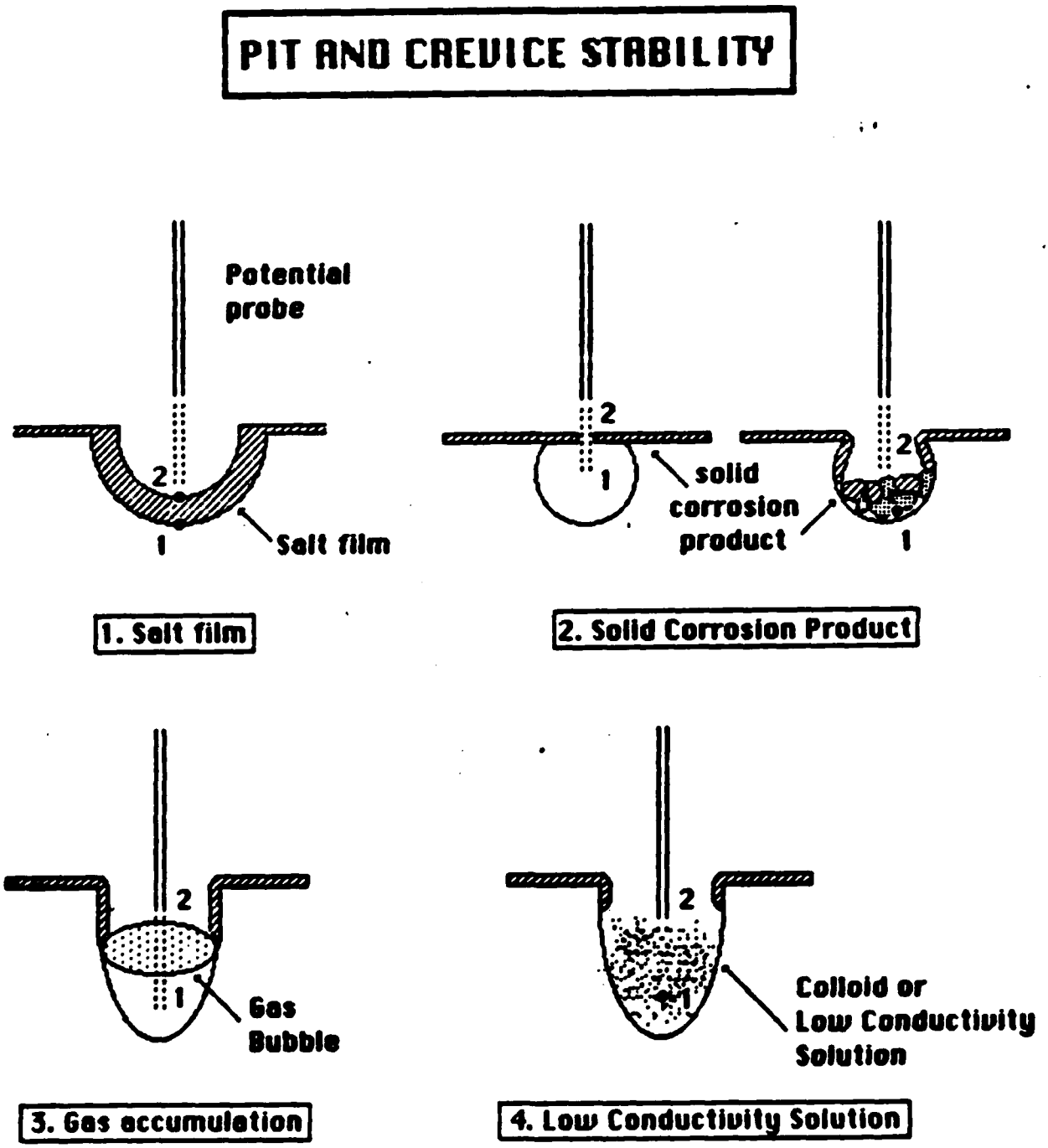


Figure 5. Schematic illustrating the different forms of constriction affecting the IR drop in the cavity. The application of a potential measuring probe for these different situations is discussed in the text.

# BUBBLE STABILITY

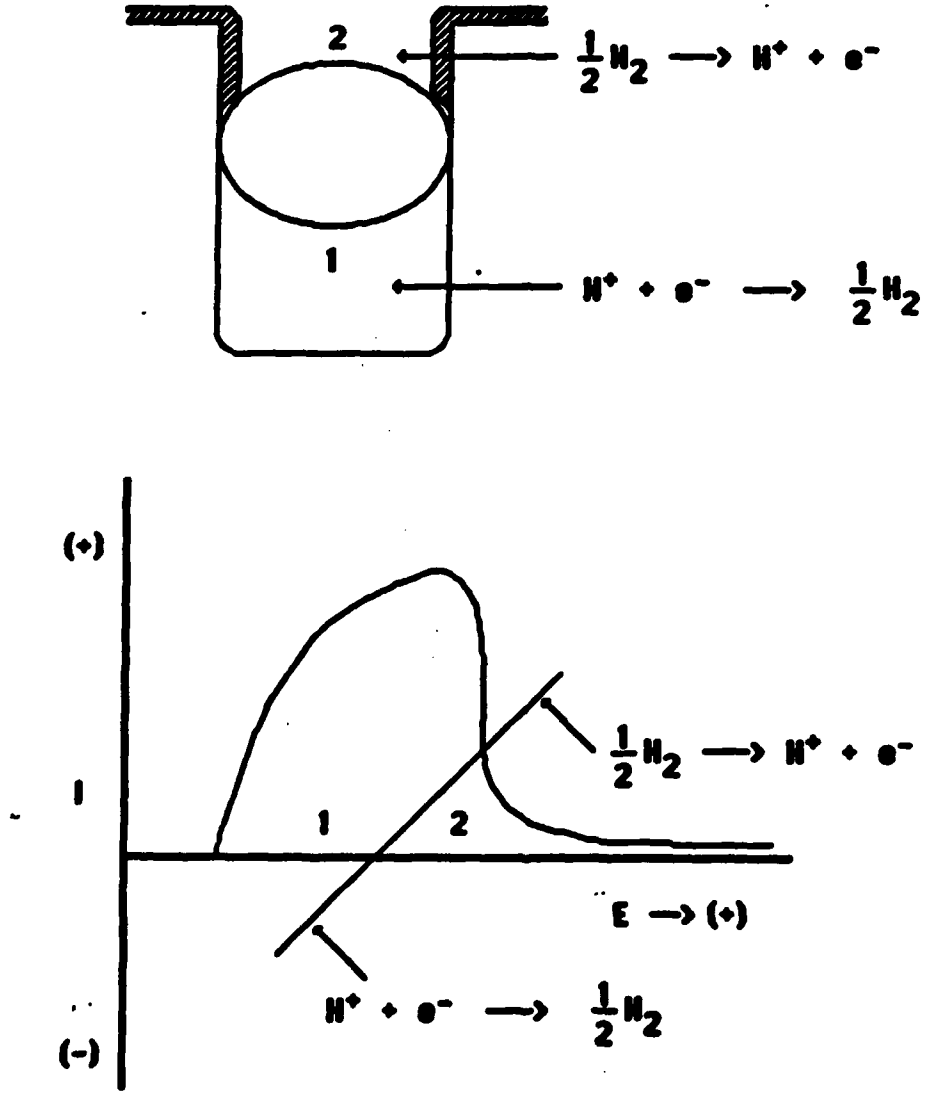


Figure 6. Schematic illustrating the relation between the polarization curves and the dynamic (chemical) stability of an inplace hydrogen gas bubble in the crevice. Increased solution viscosity also contributes to the (mechanical) stability.

DEPARTMENT OF THE NAVY
OFFICE OF NAVAL RESEARCH
ARLINGTON, VIRGINIA 22217

IN REPLY REFER TO

BASIC DISTRIBUTION LIST

Technical and Summary Reports 1985

| Organization | Copies |
|---|---|
| Defense Documentation Center<br>Cameron Station<br>Alexandria, VA 22314 | 12 |
| Office of Naval Research<br>Department of the Navy<br>800 N. Quincy Street<br>Arlington, VA 22217<br>Attn: Code 431 | 3 |
| Naval Research Laboratory<br>Washington, DC 20375<br>ATTN: Codes 6000<br>6300<br>2627 | 1<br>1<br>1 |
| Naval Air Development Center<br>Code 606<br>Warminster, PA 18974<br>ATTN: Dr. J. DeLuccia | 1 |
| Commanding Officer<br>Naval Surface Weapons Center<br>White Oak Laboratory<br>Silver Spring, MD 20910<br>ATTN: Library | 1 |
| Naval Oceans Systems Center<br>San Diego, CA 92132<br>ATTN: Library | 1 |
| Naval Postgraduate School<br>Monterey, CA 93940<br>ATTN: Mechanical Engineering Department | 1 |
| Naval Air Systems Command<br>Washington, DC 20360<br>ATTN: Code 310A<br>Code 5304B | 1<br>1 |
| Naval Sea System Command<br>Washington, DC 20362<br>ATTN: Code 05R | 1 |
| Naval Air Propulsion Test Center<br>Trenton, NJ 08628<br>ATTN: Library | 1 |
| Naval Construction Battallion<br>Civil Engineering Laboratory<br>Port Hueneme, CA 93043<br>ATTN: Materials Division | 1 |
| Naval Electronics Laboratory<br>San Diego, CA 92152<br>ATTN: Electron Materials Sciences Division | 1 |
| Naval Missile Center<br>Materials Consultant<br>Code 3312-1<br>Point Mugu, CA 92041 | 1 |
| Commander<br>David W. Taylor Naval Ship Research and Development Center<br>Bethesda, MD 20084 | 1 |
| Naval Underwater System Center<br>Newport, RI 02840<br>ATTN: Library | 1 |
| Naval Weapons Center<br>China Lake, CA 93555<br>ATTN: Library | 1 |
| NASA<br>Lewis Research Center<br>21000 Brookpark Road<br>Cleveland, OH 44135<br>ATTN: Library | 1 |
| National Bureau of Standards<br>Washington, DC 20234<br>ATTN: Metals Science and Standards Division<br>Ceramics Glass and Solid State Science Division<br>Fracture and Deformation Div. | 1<br>1<br>1 |

Naval Facilities Engineering Command
Alexandria, VA 22331
ATTN: Code 03 1

Scientific Advisor
Commandant of the Marine Corps
Washington, DC 20380
ATTN: Code AX 1

Army Research Office
P. O. Box 12211
Triangle Park, NC 27709
ATTN: Metallurgy & Ceramics Program 1

Army Materials and Mechanics Research Center
Watertown, MA 02172
ATTN: Research Programs Office 1

Air Force Office of Scientific Research/NE
Building 410
Bolling Air Force Base
Washington, DC 20332
ATTN: Electronics & Materials Science Directorate 1

NASA Headquarters
Washington, DC 20546
ATTN: Code RRM 1

General Electric Company
P.O. Box 7722
Philadelphia, PA 19101

Defense Metals and Ceramics Information Center
Battelle Memorial Institute
505 King Avenue
Columbus, OH 43201 1

Metals and Ceramics Division
Oak Ridge National Laboratory
P.O. Box X
Oak Ridge, TN 37380 1

Los Alamos Scientific Laboratory
P.O. Box 1663
Los Alamos, NM 87544
ATTN: Report Librarian 1

Argonne National Laboratory
Metallurgy Division
P.O. Box 229
Lemont, IL 60439 1

Brookhaven National Laboratory
Technical Information Division
Upton, Long Island
New York 11973
ATTN: Research Library 1

Library
Building 50, Room 134
Lawrence Radiation Laboratory
Berkeley, CA 1

Send ONE COPY to each unless otherwise indicated.

036 (4315)

Supplemental Distribution List Mar 1987

Prof. I.M. Bernstein
Dept. of Metallurgy and Materials Science
Carnegie-Mellon University
Pittsburgh, PA 15213

Prof. H.K. Birnbaum
Dept. of Metallurgy & Mining Eng.
University of Illinois
Urbana, Ill 61801

Prof. H.W. Pickering
Dept. of Materials Science and Eng.
The Pennsylvania State University
University Park, PA 16802

Prof. D.J. Duquette
Dept. of Metallurgical Eng.
Rensselaer Polytechnic Inst.
Troy, NY 12181

Prof. J.P. Hirth
Dept. of Metallurgical Eng.
The Ohio State University
Columbus, OH 43210

Prof. H. Leidheiser, Jr.
Center for Coatings and Surface Research
Sinclair Laboratory, Bld. No. 7
Lehigh University
Bethlehem, PA 18015

Dr. M. Kendig
Rockwell International - Science Center
1049 Camino Dos Rios
P.O. Box 1085
Thousand Oaks, CA 91360

Prof. R. A. Rapp
Dept. of Metallurgical Eng.
The Ohio State University
Columbus, OH 43210

Profs. G.H. Meier and F.S.Pettit
Dept. of Metallurgical and Materials Eng.
University of Pittsburgh
Pittsburgh, PA 15261

Dr. W. C. Moshier
Martin Marietta Laboratories
1450 South Rolling Rd.
Baltimore, MD 21227-3898

Prof. P.J. Moran
Dept. of Materials Science & Eng.
The Johns Hopkins University
Baltimore, MD 21218

Prof. R.P. Wei
Dept. of Mechanical Engineering and Mechanics
Lehigh University
Bethlehem, PA 18015

Prof. W.H. Hartt
Department of Ocean Engineering
Florida Atlantic University
Boca Raton, Florida 33431

Dr. B.G. Pound
SRI International
333 Ravenswood Ave.
Menlo Park, CA 94025

Prof. C.R. Clayton
Department of Materials Science & Engineering
State University of New York
Stony Brook
Long Island, New York 11794

Prof. Boris D. Cahan
Dept. of Chemistry
Case Western Reserve Univ.
Cleveland, Ohio 44106

Dr. K. Sadananda
Code 6390
Naval Research Laboratory
Washington, D.C. 20375

Prof. M.E. Orazem
Dept. of Chemical Engineering
University of Virginia
Charlottesville, VA 22901

Mr. T.W. Crooker
Code 6310
Naval Research Laboratory
Washington, D.C. 20375

Prof. G.R. St. Pierre
Dept. of Metallurgical Eng.
The Ohio State University
Columbus, OH 43210

Prof. G. Simkovich
Dept. of Materials Science & Eng.
The Pennsylvania State University
University Park, PA 16802

Dr. E. McCafferty
Code 6310
Naval Research Laboratory
Washington, D. C. 20375

END

DATE

FILMED

6-1988

DTIC.